Ordered Surface Structure in $La_{1-x}Ca_xMnO_3$ Films

H. B. Peng, B. R. Zhao,* Z. Xie, Y. Lin, B. Y. Zhu, Z. Hao, H. J. Tao, B. Xu, C. Y. Wang, H. Chen, and F. Wu

National Laboratory for Superconductivity, Institute of Physics and Center for Condensed Matter Physics, Chinese Academy of Sciences, Beijing 100080, China

(Received 11 August 1998)

The surface of $La_{1-x}Ca_xMnO_3$ (LCMO) films with $x = 0.1$, 0.33, 0.5, and 0.66 has been studied; a highly ordered grain pattern induced by strain is observed in films with $x = 0.5$ and 0.66. The strain is identified to result from thermal expansion mismatch between substrate and film, and thermal expansion anomaly may exist at a high temperature induced by possible phase transition in LCMO with $x = 0.5$ and 0.66. Such phenomenon is arresting on film growth and understanding colossal magnetoresistance materials as well as providing a new way to make ordered structures for application. [S0031-9007(98)08175-7]

PACS numbers: 68.55.–a, 65.70.+y, 75.70.–i

There has been a surge of interest in perovskite manganites since the discovery of the colossal magnetoresistance (CMR) phenomenon [1,2]. The prototype material $La_{1-x}Ca_xMnO_3$ (LCMO) shows rich phases [3,4] with a variation of calcium concentration x. Experimental and theoretical works [4–7] have been done in order to understand the physics in LCMO. So far, the investigation of LCMO has been mostly performed within the concentration range $x < 0.5$, where large magnetoresistance effects were observed. Particularly, for the films of LCMO, research is nearly focused on the magnetotransport property of optimally doped $La_{0.67}Ca_{0.33}MnO_3$. However, film growth and surface morphology have attracted numerous studies in both semiconductor [8] and perovskite oxide systems, because each material may have its own growth mode and it can reveal some deep features of the material. Also, there is broad interest in the search for new methods to fabricate ordered microstructures for their importance in potential applications [9–13]. Because of their rich phases, LCMO films may have distinctive growth characteristics corresponding to different x. But little work has been done on the film growth of LCMO within different phase regions. In the present work, we focus on the surface structure of LCMO films with different phases under various deposition conditions. The surface morphology of a series of LCMO films with different x ($x = 0.1$, 0.33, 0.5, and 0.66) was studied, and spontaneous formation of long range ordered surface structure was observed in films with $x = 0.5$ and $x = 0.66$, for which charge ordering states have been reported [14,15]. The unique feature of this structure is that chains of nanodots regularly spread throughout the film surface. Thus it opens a new window for the patterning of nanometer-scale structures.

Targets of LCMO with $x = 0.1$, 0.33, 0.5, and 0.66 were prepared by a conventional solid reactive method. Powder x-ray diffraction analysis showed single-phase patterns, and inductively coupled plasma atomic emission spectrometry (ICP) analysis showed stoichiometric composition. Films were prepared by pulsed laser deposition (PLD) with a laser fluence about 1.5 J/cm^2. The thin films with $x = 0.1$ (L1-1), $x = 0.33$ (L3-1), $x = 0.5$ (L5-1), and $x = 0.66$ (L6-1) were grown on substrate (100) $SrTiO_3$ (STO) by the same process. After deposition at 800 °C, the films were heated to 900 °C in 5 min, at which they were annealed for 20 min. The films were then cooled down to room temperature in 160 min. X-ray diffraction analysis showed that all of the samples were (001) oriented. The metal composition of the films was measured by scanning-electron-microscopy energy-dispersive spectroscopy (SEM-EDS) analysis, and it showed the same as targets. Each film has nearly the same thickness of ~1600 Å.

The atomic force microscopy (AFM) images of the films are shown in Fig. 1. On the surface of the film with $x = 0.33$ (L3-1), grains are uniformly distributed

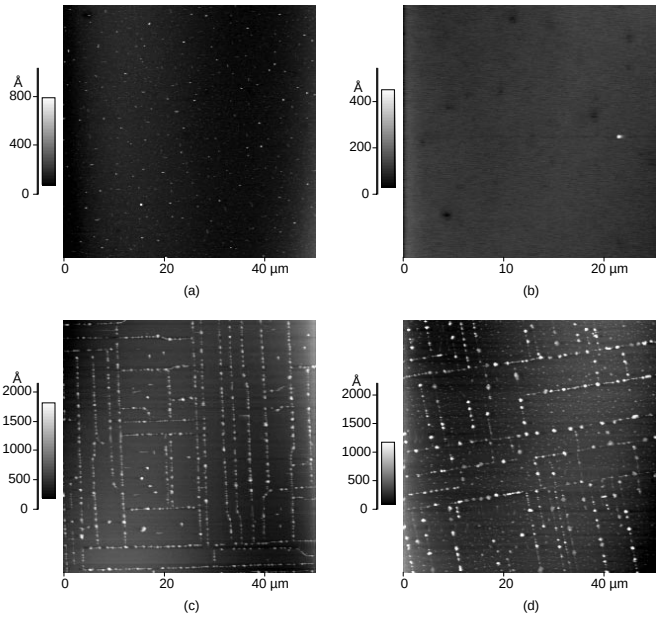

FIG. 1. AFM images of the films with (a) $x = 0.33$ (L3-1), (b) $x = 0.1$ (L1-1), (c) $x = 0.5$ (L5-1), and (d) $x = 0.66$ (L6-1). They were annealed at 900 °C for 20 min after deposition at 800 °C, and then cooled down to room temperature in 160 min.

 0031-9007/99/82(2)/362(4)$15.00

(Fig. 1a); for the film with $x = 0.1$ (L1-1), the surface is rather flat with a few grains (Fig. 1b). In contrast to that, spectacular features are observed on the surface of the films with $x = 0.5$ (L5-1) (Fig. 1c) and $x = 0.66$ (L6-1) (Fig. 1d): most of the grains are aligned in vertical and parallel rows. The rows are along the $\langle 100 \rangle$ directions of the substrate STO. This pattern can even be observed by an optical microscope, under which parallel and vertical necklacelike chains of grains spread throughout the whole film surface. However, no similar ordered structure was found on the substrate STO surface before depositing films. Some grain chains are longer than 100 μm, and the intervals between chains are of the order of μm. Note that the rectangular areas enclosed by the grain chains are rather flat, and some are completely free of grains. This suggests that some atoms from these areas were redistributed to form the grain chains during the process of growth.

Figure 2a shows the details of a grain chain on the surface of $x = 0.5$, sample L5-1. The grains have the height of about 1000 Å and the width of about several thousand angstrom, while the average roughness of the flat part between chains is about 19 Å. From a more detailed image of the two grains on the chain, we find that there is a crevice between grains. The scanning electron microscopy image (Fig. 2b) shows clearly that below each grain chain there is a cracked line. From the shape of the grains, we can see that the grains grow along the cracks. By SEM-EDS analysis, we found that the composition of the grains is the same as that of the film. Moreover, it seems that the grains are in the form of single crystals.

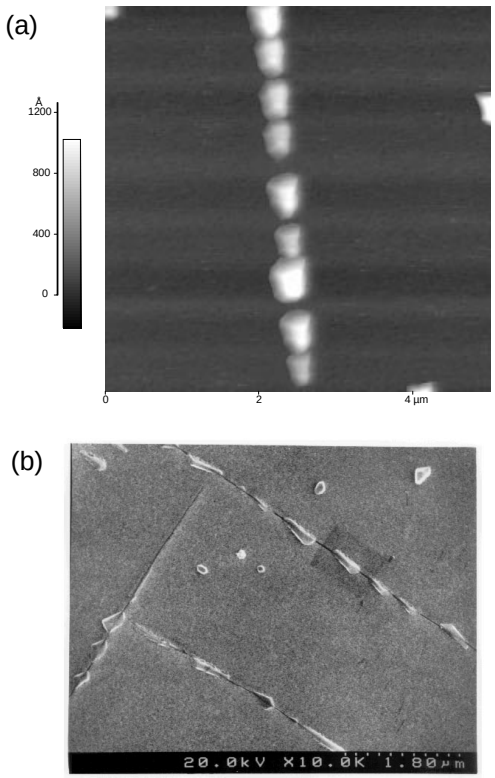

FIG. 2. (a) AFM image of a grain chain on the surface of the $x = 0.5$ film L5-1; (b) SEM image of cracks and grains in the $x = 0.5$ film L5-1.

As far as we know, there is no report of such a surface pattern on LCMO films, although a similar ordered structure induced by the surface strain has been observed [8] in epitaxial semiconductor films on prestructured substrates. It is believed that the strain and defect at surface can provide energetically favorable sites for grain location and they are common driving forces for the grain alignment [8]. In our samples, the strain could result in parallel and vertical cracks (Fig. 2b), and grains are inclined to nucleate on such places. Thus the ordered surface structure is formed. On the other hand, it was found that for the films with $x = 0.5$, when the film thickness is less than 1300 Å, no patterned surface can be observed. This is also evidence that the surface pattern in our films is induced by strain since, in the usual case, the effect of strain depends on the film thickness. But what is the origin of the strain in our films? A possible source of strain is the lattice mismatch between the substrate and the film. The lattice mismatch between LCMO and STO is enlarged as x increases (seen in Table I). However, we got the same result in LCMO films grown on (100) $LaAlO_3$, for which the lattice mismatch to LCMO becomes smaller as x increases. It is obvious that the lattice mismatch could not be the main reason for the patterned structure.

Note that, for the film with $x = 0.1$ or 0.33, no patterned surface structure can be observed although we varied the deposition condition systematically as well as the film thickness, but the pattern is very reproducible in the film with $x = 0.5$ or 0.66 under certain deposition conditions. It seems that the strain should be attributed to some inherent features of LCMO with $x = 0.5$ and 0.66. Previously, one type of strain pattern in $Bi_{0.2}Ca_{0.8}MnO_3$ [16] was observed at 130 K when charge ordering occurred, which was explained by the intrinsic strain due to the Jahn-Teller effect of Mn^{3+}. But, in our work, the strain exists at a high temperature unimaginable for charge ordering. Hence there must be other reasons contributing to the strain.

Previously, different ordered surface structures induced by the mismatch of thermal expansion coefficients between substrate and film were reported [9,17]. We think that the pattern in our work may also result from the

TABLE I. Lattice mismatch of substrate (100) $SrTiO_3$ and (100) $LaAlO_3$ with the film of different x, respectively.

	$x = 0.1$	$x = 0.33$	$x = 0.5$	$x = 0.66$
$SrTiO_3$	+0.4%	+1.1%	+1.6%	+3.3%
$LaAlO_3$	−2.5%	−1.8%	−1.3%	+0.4%

thermal expansion mismatch between STO and LCMO. When the temperature is changed, the relative expansion or contraction between film and substrate due to their different thermal expansion coefficients causes strain in the film. The accumulated stress σ, when the temperature is changed from T_0 to T_1, can be written as

$$\sigma = \left| E_f \int_{T_0}^{T_1} (\alpha_f - \alpha_s)\, dT \right| . \qquad (1)$$

Here E_f is the Young's modulus of the film; α_f and α_s are the thermal expansion coefficients of the film and the substrate, respectively (they are functions of temperature T). Considering a given film thickness t, when the accumulated stress σ reaches a critical value σ_{cr}, regularly spaced cracks will appear to release the energy. σ_{cr} is given [18] by

$$\sigma_{\mathrm{cr}} = K_{Ic}/\sqrt{2t}\,, \qquad (2)$$

where K_{Ic} is the fracture toughness of the film. If the temperature is changed rapidly, the stress σ cannot be relaxed and exceeds σ_{cr}. Then cracks will be formed. But if the temperature is changed slowly enough, the stress can be relaxed and will not result in cracks. On the other hand, under a constant stress σ, regularly spaced cracks will appear if the film thickness exceeds a critical value t_{cr}.

In the present case, since the grains grow at high temperature, the cracks should be formed due to thermal expansion mismatch when the films are heated from 800 to 900 °C after deposition. To confirm that, we prepared three more films with $x = 0.5$: (1) after deposition at 800 °C, heated to 900 °C in 5 min, and annealed for 20 min (the same process as L5-1), then slowly cooled down to room temperature in 16 h (L5-2); (2) deposited at 800 °C, then slowly cooled down to room temperature in 16 h after being annealed at 800 °C for 80 min (L5-3); (3) deposited at 800 °C, then quickly cooled down to room temperature in 20 min after being annealed at 800 °C for 80 min (L5-4). In the film L5-2 (Fig. 3a), with long cooldown time, the grains grow more closely along the lines and, in some places, the grains are connected into lines. Compared with L5-1, the result of L5-2 confirms that the cracks appeared before cooldown, i.e., cracks mainly occurred when the temperature was increased from 800 to 900 °C, and then the grains grew along the cracks. In the film L5-3 (Fig. 3b), no pattern is observed, and grains are randomly distributed. Because, in this case, we didn't raise the temperature from 800 to 900 °C, no cracks were induced by thermal expansion mismatch, and grains lacked energetically favorable sites to nucleate. On the other hand, with slow cooldown speed, the stress induced by relative contraction between the film and the substrate was relaxed, thus no cracks appeared in L5-3 during cooldown. While in the sample L5-4 with a short cooldown time (Fig. 3c), the accumulated stress caused patterned cracks; but with a short time to stay

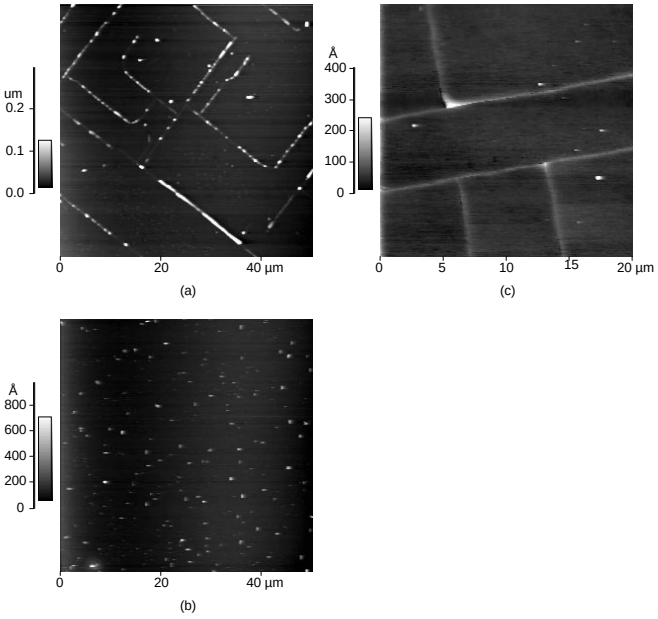

FIG. 3. AFM images of $x = 0.5$ films with (a) annealed at 900 °C for 20 min after deposition at 800 °C, then slowly cooled down to room temperature in 16 h (L5-2); (b) annealed at 800 °C for 80 min after deposition at 800 °C, then slowly cooled down to room temperature in 16 h (L5-3); (c) annealed at 800 °C for 80 min after deposition at 800 °C, then quickly cooled down to room temperature in 20 min (L5-4).

at high temperature, grains had not been driven to align along the cracks yet. Combining the results of L5-1 to L5-4, we can conclude that the surface pattern results from the strain induced by the difference in thermal expansion coefficients between film and substrate at high temperature. In short, the cracks occurred while changing temperature, and then the grains grew into chains during the anneal process.

It should be further noted that large difference of thermal expansion may exist between different temperature ranges in LCMO with $x = 0.5$. Although we can avoid cracks at a speed of about 100 °C/h during cooling down from 800 °C, cracks can still appear during heating from 800 to 900 °C at a slower speed of about 20 °C/h. This implies that the strain caused in that high temperature region is large and cannot be easily relaxed, different from the case when the films were cooled down from 800 °C. We also found that, from 800 to 900 °C, the accumulated stress σ is large enough to cause cracks only with a small change of temperature. From Eq. (1), it is obvious that there must be a large mismatch of thermal expansion coefficients between the film and substrate at this temperature range. Even an anomaly of thermal expansion coefficient may exist in $x = 0.5$ films at that temperature range.

We also found the same situation in the films with $x = 0.66$. It is interesting that, with the variation of calcium concentration x, there is such a large difference in thermal expansion property. It needs to be mentioned

that, in a relatively low temperature range, with $x = 0.5$ or 0.66, LCMO is in an antiferromagnetic state coexisting with charge ordering, but it is ferromagnetic with $x = 0.1$ or 0.33 [4]. Does the different phase within a different range of x account for such a difference in thermal property? Furthermore, as far as LCMO with $x = 0.5$ or 0.66 is concerned, what leads to the abnormal thermal expansion at high temperature? It should be considered that some phase transitions can contribute to thermal expansion anomaly. For LCMO, a clear anomaly of thermal expansion has been reported [19] at the phase transition point to charge ordering state. Hence, one possibility is that, in LCMO with $x = 0.5$ and 0.66, a certain type of phase transition may occur at high temperature (for example, a structure phase change) and lead to some anomalous parts of the thermal expansion coefficient. Unfortunately, little work has been done to investigate the properties of LCMO, such as thermal expansion at a high temperature region. However, such work is necessary to understand the nature of CMR materials more deeply.

In summary, the surface morphology of a series of LCMO films with different calcium concentration x prepared by PLD has been studied. An ordered surface pattern with grains being aligned along vertical and parallel lines was observed in the films with $x = 0.5$ and $x = 0.66$, and the pattern was identified to be induced by strain resulting from the large difference in thermal expansion coefficients between film and substrate. Furthermore, we suggest that there should be an anomaly of thermal expansion at high temperature, possibly associated with phase transition, in LCMO with $x = 0.5$ and 0.66. Such a phenomenon is not only interesting in the film growth and the mechanics of films, but also presents a new perspective to understand the intrinsic of CMR materials. In addition, because the growth of the grain pattern can be controlled by adjusting deposition condition, it provides a novel way to make ordered structures for application. Compared with the attempts [10–13] for patterning ordered structures through complex technique in postgrowth process, the present method is simple and unique, and the surface pattern is spontaneously formed during the *in situ* process of film growth. Thus it holds promise in making ordered nanodot structures for potential applications.

We thank Dr. C. L. Chen and Dr. X. L. Dong for helpful discussions.

*Corresponding author.

[1] R. von Helmolt, J. Wecker, B. Holzapfel, M. Schultz, and K. Samwer, Phys. Rev. Lett. **71**, 2331 (1993).
[2] S. Jin *et al.*, Science **264**, 413 (1994).
[3] P. Schiffer, A. P. Ramirez, W. Bao, and S. W. Cheong, Phys. Rev. Lett. **75**, 3336 (1995).
[4] A. J. Millis, Nature (London) **392**, 147 (1998).
[5] C. Zener, Phys. Rev. **82**, 403 (1951); P. G. de Gennes *ibid.* **118**, 141 (1960).
[6] G. M. Zhao, K. Conder, H. Keller, and K. A. Müller, Nature (London) **381**, 676 (1996).
[7] J. S. Zhou and J. B. Goodenough, Phys. Rev. Lett. **80**, 2665 (1998).
[8] S. Y. Shiryaev, F. Jensen, J. L. Hansen, J. W. Petersen, and A. N. Larsen, Phys. Rev. Lett. **78**, 503 (1997).
[9] N. Bowden, S. Brittain, A. G. Evans, J. W. Hutchinson, and G. M. Whitesides, Nature (London) **393**, 146 (1998).
[10] J. I. Martin *et al.*, Appl. Phys. Lett. **72**, 255 (1998).
[11] K. S. Johnson *et al.*, Science **280**, 1583 (1998).
[12] C. Chappert *et al.*, Science **280**, 1919 (1998).
[13] R. J. Jackman, S. T. Brittain, A. Adams, M. G. Prentiss, and G. M. Whitesides, Science **280**, 2089 (1998).
[14] C. H. Chen and S.-W. Cheong, Phys. Rev. Lett. **76**, 4042 (1996).
[15] S. Mori, C. H. Chen, and S.-W. Cheong, Nature (London) **392**, 473 (1998).
[16] Y. Murakami, D. Shindo, H. Chiba, M. Kikuchi, and Y. Syono, Phys. Rev. B **55**, 15 043 (1997).
[17] D. K. Fork *et al.*, Appl. Phys. Lett. **58**, 2432 (1991).
[18] M. D. Thouless, J. Am. Ceram. Soc. **73**(7), 2144 (1990).
[19] M. R. Ibarra *et al.*, Phys. Rev. B **56**, 8252 (1997).